Applied Energy 100 (2012) 193–204

Contents lists available at SciVerse ScienceDirect

Applied Energy

journal homepage: www.elsevier.com/locate/apenergy

Optimal design and control of solar driven air gap membrane distillation desalination systems

Yih-Hang Chen *, Yu-Wei Li, Hsuan Chang

Department of Chemical and Materials Engineering, Tamkang University, Danshui Dist., New Taipei City 25137, Taiwan

ARTICLE INFO

Article history:
Received 19 December 2011
Received in revised form 28 February 2012
Accepted 1 March 2012
Available online 30 March 2012

Keywords:
Air gap membrane distillation
Desalination
ACM software
Optimal design
Control
TAC

ABSTRACT

A solar heated membrane distillation desalination system is constructed of solar collectors and membrane distillation devices for increasing pure water productivity. This technically and economically feasible system is designed to use indirect solar heat to drive membrane distillation processes to overcome the unstable supply of solar radiation from sunrise to sunset. The solar heated membrane distillation desalination system in the present study consisted of hot water storage devices, heat exchangers, air gap membrane distillation units, and solar collectors. Aspen Custom Molder (ACM) software was used to model and simulate each unit and establish the cost function of a desalination plant. From Design degree of freedom (DOF) analysis, ten design parameters were investigated to obtain the minimum total annual cost (TAC) with fixed pure water production rate. For a given solar energy density profile of typical summer weather, the minimal TAC per 1 m^3 pure water production can be found at 500 W/m^2 by varying the solar energy intensity. Therefore, we proposed two modes for controlling the optimal design condition of the desalination plant; day and night. In order to widen the operability range of the plant, the sensitivity analysis was used to retrofit the original design point to lower the effluent temperature from the solar collector by increasing the hot water recycled stream. The simulation results show that the pure water production can be maintained at a very stable level whether in sunny or cloudy weather.

1. Introduction

Due to global warming effects and a growing world population, the demand on water resources has been redistributed. Scientists have paid much attention to an efficient and environmentally friendly way to generate desalinated water. Desalination can be taken as a candidate method to meet part of the world's redistributed water and increasing fresh water needs due to the abundance of seawater. Desalination technologies are used worldwide and can produce potable water, and zero carbon emission, but they waste energy [1–5]. Commercial desalination plants can be classified into several types: First one is phase change/thermal technology, i.e., multi-stage flash. Second one is membrane separation, i.e., reverse osmosis (RO) [6]. Other types include vapor compression (VC) [7,8] and electrodialysis (ED). In order to overcome the drawbacks of existing commercial technologies which are; huge power supply and a lot of energy waste, combining renewable solar energy and membrane distillation for desalination systems has become a popular technology in recent years [3,9–18].

Solar heated membrane distillations are categorized into four types: Direct contact membrane distillation (DCMD), air gap membrane distillation (AGMD), sweeping gas membrane distillation (SGMD), and vacuum membrane distillation (VMD). Air gap membrane distillations [19–21] have the lowest energy consumption per unit distillate water generation of these membrane distillation modules. Many researchers have used mathematical models to simulate and understand the mass and heat transfer phenomena of the AGMD module to find the key design and operating variables for increasing water permitted flux [12,21–23]. Chang et al. [12,24] and Ben Bacha et al. [21] built mathematical models of all units and discussed the operation and control issues of the solar driven AGMD desalination plant. Gálvez et al. [25] designed a 50 m^3/day capacity water production from seawater desalination by innovative solar-powered membrane. Guillen-Burrieza et al. [26] built a pilot system for solar AGMD desalination. These two articles are based on minimizing the specific energy consumption per unit distillate water flowrate to evaluate the system operating performance. Song et al. [27] constructed a small pilot plant of membrane distillation desalination system and operated successfully on a daily basis for 3 months. Most of their work focuses on how to operate the system with high thermal efficiency without taking the plant capital cost into consideration. But total cost of plants should include the capital and energy cost. The time-varying system for unpredictable solar radiation intensity made the analysis of the total plant cost difficult. In this work, the minimum plant cost with a totally controllable control structure design is discussed.

* Corresponding author. Tel.: +886 226215656x3283; fax: +886 226209887.
E-mail address: yihhang@mail.tku.edu.tw (Y.-H. Chen).

0306-2619/$ - see front matter © 2012 Elsevier Ltd. All rights reserved.
http://dx.doi.org/10.1016/j.apenergy.2012.03.003

Nomenclature

A_{SC}	surface area of the solar collector (m^2)
A_{MD}	membrane area (m^2)
$A_{HX\text{-}1}$	heat transfer area of the heat exchange (m^2)
B	absorption coefficient (0.8)
C_B	purchased cost of major unit ($)
C_p	purchased cost ($)
C_P	heat capacity (J/kg K)
C_{pc}	heat capacity of the absorbed plate (460 J/kg K)
C_{pf}	heat capacity of the fluid in the absorbed plate (4180 J/kg K)
D	distillate water flowrate (kg/h)
D_h	hydraulic diameter (m)
F	volumetric flowrate (m^3/h)
F_L	coefficient of the pipe length (1)
F_M	material cost factor (–)
F_p	pressure cost factor (–)
F_T	pump type factor (–)
H	pump head (m)
h	heat convention coefficient (W/m^2 K)
h_{vap}	heat of vaporization (J/kmol)
I	solar radiation intensity (W/m^2)
k	heat conductivity coefficient (J/s m^2 K)
L	length of unit (m)
L_{MD}/W_{MD}	aspect ratio of the membrane (–)
L_{SC}/W_{SC}	aspect ratio of the solar collector (–)
M_c	weight of the absorbed plate (kg)
M_{cl}	mass of fluid in the cold side (kg)
M_{hl}	mass of fluid in the hot side (kg)
M_f	mass of fluid in the fluid channel of the absorbed plate (kg)
M_S	mass of the storage tank (kg)
M_w	mass of fluid in the storage tank (kg)
mw	molecular weight (18.015 kg/kmol)
m_{cl}	mass flowrate in the cold side of the heat exchanger (kg/s)
m_f	mass flowrate in the absorbed plate (kg/s)
mf_h	the entrance mass flowrate from heat exchanger to storage tank (kg/s)
m_{fs}	the entrance mass flowrate from absorbed plate to storage tank (kg/s)
m_{hl}	mass flowrate in the hot side of the heat exchanger (kg/s)
N	molar flux (kmol/m^2 s)
P	pressure (Pa)
P_{lnair}	pressure of log mean temperature
Pr	Prandtl number (–)
Q	heat flux (kJ/m^2s)
R	gas constant (8314.3 Pa m^3/kmol K)
Re	reynolds number (–)
S	equipment size coefficient(–)
T	temperature (K)
T_a	ambient temperature (25 °C)
T_c	the temperature of the absorbed plate (°C)
$T\_\{cl\}$	the cold side temperature of the heat exchanger (°C)
T_f	the temperature of the fluid in the absorbed plate (°C)
T_{gm1}	interface of membrane and hot fluid (°C)
T_{gm2}	interface of membrane and air gap (°C)
T_{hl}	the hot side temperature of the heat exchanger (°C)
T_{m1}	interface of condensate water and metal wall (°C)
T_{m2}	interface of metal and cold fluid (°C)
T_w	the temperature of the storage tank (°C)
U	overall heat transfer coefficient (280 W/m^2 K)
V	velocity (m/s)
W	width of unit (m)

Italic

δ	thickness (m)
μ	viscosity (kg/m s)
ρ	density (kg/m^3)
Ω	stands for optimization variables

Subscript

ag	air gap layer
cl	cold fluid
conl	condensate fluid
D	design of freedom
D-1	storage tank 1
f	the interface between condensate and air gap layer
gm	internal layer of the membrane
hl	hot fluid
HX-1	heat exchanger
MD	membrane
m	metal layer
No.	stream no.
R	recyclewater flowrate
SC	solar collector
sea	seawater flowrate

We have addressed and solved the design and control framework problems of solar driven AGMD desalination systems. In Section 2, we built the mathematical model of each unit of the desalination process. In Section 3, the "pseudo steady-state method" was used to determine the optimal steady-state TAC design and operating points for different solar radiation intensities. In Section 4, sensitivity analysis was used to determine the control-pairing of the desalination plant. In Section 5, the control structure was built and was used to test the control performance under different solar radiation scenarios.

2. Solar driven air gap membrane distillation desalination systems

2.1. Process description

A solar heated membrane distillation desalination system can be constructed of solar collectors and membrane distillation devices for increasing pure water productivity. This technically and economically feasible system can be designed to use indirect solar heat to drive membrane distillation processes to overcome the unstable supply of solar radiation from sunrise to sunset. The solar heated membrane distillation desalination system in the present study consists of two parts. One is cold seawater cycle path; the other is hot water recycled path. The process flow diagram is shown in Fig. 1. The seawater (Stream1) is pumped into the cold side of AGMD (Air gap membrane distillation). The AGMD module consists of hot water flow channel, cold water flow channel, a hydrophobic porous membrane and an air gas layer which is located between the membrane and cold seawater flow channel. The membrane is made of Polytetrafluoro Ethylene (PTFE) and the properties of the membrane are shown in Table 1. The effluent of the cold seawater (Stream 2) flows into the shell side of the heat exchanger (HX-1) and is heated by the hot recycled water in the tube side. The heat exchange effluent stream (Stream 3) from the shell side flows into the hot flow channel of the AGMD unit. Because of the hydrophobic property of the porous membrane, water

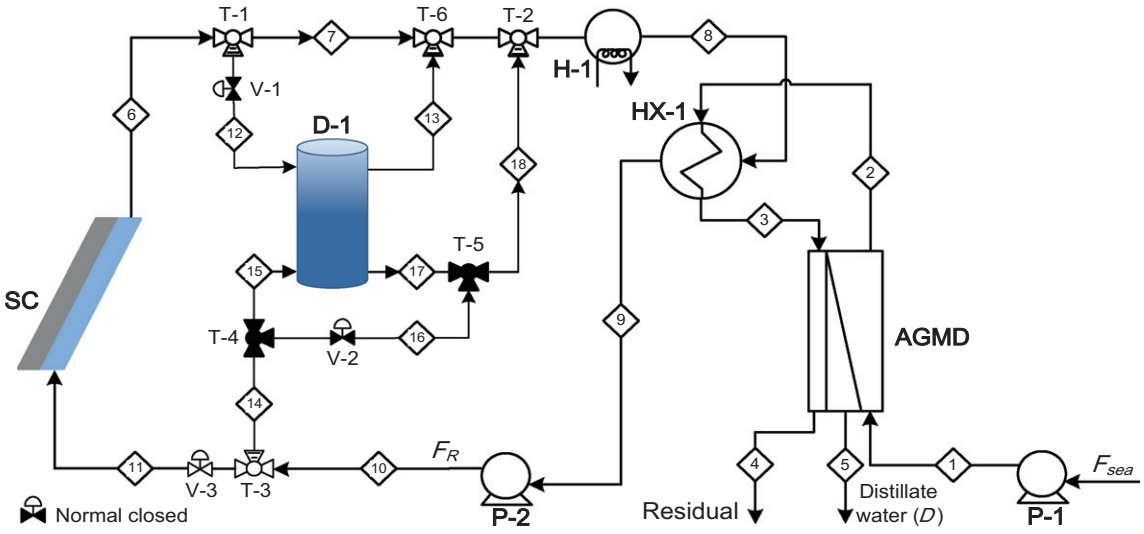

Fig. 1. Process flow diagram of solar heated membrane distillation desalination systems.

Table 1
The physical properties of the PTFE porous membrane [12,17].

Membrane area	m^2	10.00
Aspect ratio (L/W)	–	20.37
Membrane thickness	mm	0.14
Porosity	–	0.77
Pore size	μm	0.2
Tortuosity	–	1.90
Thermal conductivity	(W/m-k)	0.173

Table 2
Modeling equations for each unit of the desalination system.

Solar collector (SC)
Energy balance equation for
Absorbing metal plate: $\frac{\partial T_c}{\partial t} = \frac{A_{SC}U}{M_c C_{pc}}\left(\frac{BI(t)}{U} + T_a(t) - T_c\right) - \frac{A_{SC}h}{M_c C_{pc}}(T_c - T_f)$ (E-1)
Heated fluid: $\frac{\partial T_f}{\partial t} = -L\frac{m_f}{M_f}\frac{\partial T_f}{\partial x} + \frac{A_{SC}h}{M_f C_{pf}}(T_c - T_f)$ (E-2)

Storage tank (D-1)
Material balance equation: $\frac{\partial M_s}{\partial t} = m_{f4} - m_{f3}$ (E-3)
Energy balance equation: $\frac{\partial T_w}{\partial t} = \frac{m_{f5}(T_{S1} - T_w) + m_{f4}(T_{S4} - T_w)}{M_w}$ (E-4)

Heat exchanger (HX-1)
Energy balance equation for
Hot fluid (shell side): $\frac{dT_{hl}}{dt} = L\frac{m_{hl}}{M_{hl}}\left(\frac{\partial T_{hl}}{\partial x}\right) - \frac{A_{HX-1}U}{M_{hl}C_{phl}}(T_{hl} - T_{cl})$ (E-5)
Cold fluid (tube side): $\frac{dT_{cl}}{dt} = \frac{m_{cl}}{M_{cl}}\left(\frac{\partial T_{cl}}{\partial x}\right) + \frac{A_{HX-1}U}{M_{cl}C_{pcl}}(T_{hl} - T_{cl})$ (E-6)

can only be transferred through the pore of the membrane in vapor form. The driving force of the water vapor flux is determined by the temperature difference between both sides of the membrane. When water vapor passes though the membrane and the air gap layer, it will condense on the wall surface of the cold seawater flow channel. The distillate water (D) effluent stream (Stream 5) from the AGMD module is collected and delivered to a storage tank.

The purpose of the hot water recycled path is to use solar energy to preheat the cold seawater. The recycled water (Stream 9) is pumped into the solar collector (SC). The recycled water adsorbs solar energy in the solar collector which increases its temperature. The effluent stream (Stream 6) from the solar collector is heated by the electrical heater (H-1) to reach the desired temperature (T_8). The hot recycled water (Stream 8) flows into the HX-1 and provides the energy to heat the cold seawater (Stream 3).

The design purpose of the storage tank (D-1) is to store the excess energy from the sun. When the level of the radiation energy from the sun changes, the bypass flowrate from T-1 is adjusted by V-1 and delivered to D-1. The D-1 tank is designed with an overflow system whereby the inlet and outlet flowrates are the same. The initial temperature of D-1 is 50 °C. The temperature of D-1 increases when more radiation energy is provided to the solar collector.

2.2. Modeling

2.2.1. Solar collector

The purpose of the solar collector is to collect energy from the sun and reduce the energy demand from the auxiliary heater. Chang et al. [12] built a mathematical model to describe the solar collector. The model assumptions are as follows: (1) The fluid velocity in each absorbed tube is the same, (2) to avoid the phase change occurring in each absorbed tube, the operating temperature of the fluid should be kept below 95 °C, (3) this unit uses the adiabatic operation, (4) no water loss from the unit. The energy balance equation for the absorbing metal plate and water are listed in Table 2 (Eqs. E-1 and E-2).

2.2.2. Storage tank

In order to overcome the unstable supply of solar radiation from sunrise to sunset, the excess energy supply to the system can be absorbed by D-1 and raise its temperature. The model assumptions are as follows: (1) This unit uses the adiabatic operation, (2) no phase change occurs in the storage tank, (3) uniform mix in the storage tank. The mass and energy balance equations are listed in Table 2 (Eqs. (E-3) and (E-4)).

2.2.3. Heat exchanger

In order to transfer the energy from the hot recycled water to the cold seawater, a countercurrent shell and tube heat exchanger is used. The model assumptions are as follows: (1) This unit uses the adiabatic operation, (2) no phase change occurs in the heat exchanger, (3) heat capacities of water in the cold and hot side of the heat exchanger are assumed to be constant. The energy balance equations for the hot and cold side of the heat exchanger are listed in Table 2 (Eqs. (E-5) and (E-6)).

2.2.4. Air gap membrane distillation (AGMD)

There are three concurrent phases in the unit. In order to describe the unit behavior, we need to record the mass and energy

modeling equations for individual parts of the AGMD unit. Avlonitis et al. [10] built a mathematical model to describe the AGMD unit. The model assumptions are as follows: (1) The phase change occurs on the interface between the hot fluid and the membrane, (2) complete mixture of the fluid in the cross-section of the fluid channels, (3) film theory is used to describe the correlation formula of the mass and heat transfer coefficient, (4) water can only be transferred through the pore of the membrane in vapor form, (5) no pressure drop occurs when vapors transfer through the pore, (6) this unit uses the adiabatic operation. The energy balance equations for this unit are listed in Table 3 [28].

Table 3
Modeling equations of the AGMD unit.

Hot fluid	
Material balance equation: $\frac{dm_{f,hl}}{dx} = -N_{gm}W$	(E-7)
Energy balance equation: $\frac{\partial T_{hl}}{\partial x} = \frac{m_{f,hl}}{M_{hl}}\frac{\partial T_{hl}}{\partial x} - \frac{(h_{hl}+N_{gm}C_{p,hl})LW}{M_{hl}C_{p,hl}}(T_{hl}-T_{gm1})$	(E-8)
where $N_{gm} = \frac{k_{gm}}{R(T_{gm1}+T_{gm2})/2}(P_{gm1}-P_{ag})$	
Membrane	
Energy balance equation: $Q_{hl} = Q_{gm} + N_{gm}h_{vap,gm1}$	(E-9)
where, $Q_{hl} = (h+N_{gm}C_{p,hl})(T_{hl}-T_{gm1})$, $Q_{gm} = (h+N_{gm}C_{p,gm})(T_{gm1}-T_{gm2})$	
Air gap	
Material balance equation: $N_{gm} = N_{ag}$	(E-10)
Energy balance equation: $Q_{gm} = Q_{ag}$	(E-11)
where $N_{ag} = \frac{k_{ag}P_{conl}}{RP_{\ln air}(T_{gm2}+T_f)/2}(P_{ag}-P_f$, $Q_{ag} = (h+N_{ag}C_{p,ag})(T_{gm2}-T_f)$	
Condensing liquid	
Material balance equation: $\frac{dm_{f,conl}}{dx} = N_{ag}W$	(E-12)
Energy balance equation: $Q_{ag} + N_{gm}h_{vap,f} = Q_{conl}$	(E-13)
where $Q_{conl} = (h+N_{ag}C_{p,conl})(T_f - T_{m1})$	
Metal layer	
Energy balance equation: $Q_{conl} = Q_m$	(E-14)
where $Q_m = h(T_{m1}-T_{m2})$	
Cool liquid	
Energy balance equation: $\frac{\partial T_{cl}}{\partial x} = \frac{m_{f,cl}}{M_{cl}}\frac{\partial T_{cl}}{\partial x} + \frac{h_{cl}LW}{M_{hl}C_{p,hl}}(T_{m2}-T_{cl})$	(E-15)
where	
$P - \exp\left(72.55 - \frac{7206.7}{T} - 7.1385\ln T + 4.04\times10^{6}T\right)$	
$h = \frac{0.065RePrk}{D_h}; D_h = 2\delta; Re = \frac{\rho v D_h}{\mu}; Pr = \frac{\mu C_p}{kmw}; V = \frac{m_f}{\rho WL}$	
$\mu = 0.001(0.9^{-0.2661\frac{25-T}{233}})^{(-1/0.2661)}; h_{vap} = 5.2053\times10^{7}(1-\frac{T}{672.3})^{0.31990.212(\frac{T}{672.3})+0.258(\frac{T}{672.3})^2}$	

Note: All the physical properties of gases and liquids can be found in Reid et al. [28].

3. Optimization

Normally, minimal total annual cost is a typical method for finding the optimal size of each piece of equipment for a system. Because of the fluctuating solar radiation, there is no steady-state operating condition for solar desalination systems. This is also a key problem in designing desalination plants. Here, we propose a "Pseudo steady-state method" to overcome these issues. This method is described as follows.

3.1. Design: degree of freedom analysis (DOF)

In order to determine the size of each piece of equipment, Luyben [29] proposed a method to investigate design degree of freedom for a plant. It is shown in the following equation:

$$N_D = N_{\text{variables}} - N_{equations} \quad (1)$$

The symbol (N_D) equates to the number of variables minus the number of equations. N_D is used to determine the unknown variables which can be used to size an individual unit. The degree of freedom analysis for solar driven AGMD desalination systems is shown in Table 4. The total number of variables and equations are ($14 + 2\ N_{SC} + 2N_{HX} + 9\ N_{MD}$) and ($4 + 2\ N_{SC} + 2N_{HX} + 9\ N_{MD}$), respectively. The design DOF can be calculated and the value is 10.

There are 10 DOFs which need to be determined by users. The variables that we chose are δ_{MD}, A_{MD}, L_{MD}/W_{MD}, δ_{SC}, A_{SC}, L_{SC}/W_{SC}, T_{sea}, T_a, F_{sea}, F_R. The variables are listed below:

(1) The aspect ratio (L_{SC}/W_{SC}) of the solar collector is set at 14 due to its optimal efficiency [30].
(2) The water flow channel thickness in the solar collector (δ_{SC}) is set at 1 cm due to the manufacturing limitation [31].
(3) The aspect ratio (L_{MD}/W_{MD}) of the AGMD is set at 20 due to the manufacturing limitation [10].
(4) The flow channel thickness of the AGMD (δ_{MD}) unit is set at 0.77 cm due to the manufacturing limitation [10].
(5) Feed temperature of the seawater (T_{sea}) is set at 25 °C.
(6) Ambient temperature (T_a) is set at 25 °C.
(7) Seawater flowrate (F_{sea}).

Table 4
Number of variables and equations for each unit of the desalination system.

	Variables		
Flows	Solar collector	F_R	1
	Storage tank	m_{f3}	1
	Heat exchanger	m_{hl}, m_{cl}	2
	MD	$m_{hl,N}$, $m_{conl,N}$, F_{sea}	$2\ N_{MD} + 1$
Temperature	Solar collector	$T_{c,N}$, $T_{f,N}$, T_a	$2N_{SC} + 1$
	Storage tank	T_w	1
	Heat exchanger	$T_{hl,N}$, $T_{cl,N}$	$2N_{HX}$
	MD	$T_{hl,N}$, $T_{gm1,N}$, $T_{gm2,N}$, $T_{f,N}$, $T_{m1,N}$, $T_{m2,N}$, $T_{cl,N}$, T_{sea}	$7N_{MD} + 1$
Holdup	Solar collector	δ_{SC}, A_{SC}, L_{SC}/W_{SC}	3
	MD	δ_{MD}, A_{MD}, L_{MD}/W_{MD}	3
Total number variables = $14 + 2\ N_{SC} + 2N_{HX} + 9\ N_{MD}$			
		Equation	
Flows		Storage tank	1
		Heat exchanger	2
		MD	$2N_{MD}$
Temperature		Solar collector	$2N_{SC}$
		Storage tank	1
		Heat exchanger	$2N_{HX}$
		MD	$7N_{MD}$
Total number equations = $4 + 2\ N_{SC} + 2N_{HX} + 9\ N_{MD}$			

(8) Recycled water flowrate (F_R).
(9) The absorbed area of the solar collector (A_{SC}).
(10) The area of AGMD (A_{MD}).

There are four DOFs which need to be determined in our system, and they are F_{sea}, F_R, A_{SC}, A_{MD}. These variables can be seen as the optimization variables which can be determined from the values of optimal operation. We will discuss the problem in a later section.

Table 5
Cost function of each unit [32,33].

Capital cost of centrifugal pumps ($USD)
$S = Q(H)^{0.5}$
$C_B = \exp(9.7171 - 0.6019[\ln(S)] + 0.0519[(S)]^2$
$C_P = F_T F_M C_B$
Capital cost of shell and tube heat exchangers ($USD)
$C_B = \exp\{11.0545 - 0.9228[\ln(A)] + 0.09861[\ln(A)]^2\}$
$F_M = a + (A/100)^b$
$F_P = 0.09803 + 0.018(P/100) + 0.0017(P/100)^2$
$F_L = 1$
$C_P = F_P F_M F_L C_B$
Capital cost of electrical heaters ($USD)
$C_p = 157.2 + 47.316Q - 0.0507Q^2$
Capital cost of porous membranes ($USD)
$C_p = 36A_m$
Capital cost of solar collector ($USD)
$C_p = 50A_{SC}$
Utility cost
Electricity cost: 0.06 ($USD/kWh)

Table 6
Optimal size of each piece of equipment for the desalination plant.

Optimal results	Unit	Value	Literature [11]	Times
F_{sea}	kg/h	29841.5	1000–1250	23.87
F_R	kg/h	14058.4	2400	5.86
A_{MD}	m^2	1628.1	40	40.70
A_{SC}	m^2	1722.2	72	23.92
A_{HX}	m^2	64.4	5	12.89
D	kg/h	2000.0	52	38.46

3.2. Objective function

For a given solar radiation intensity, the objective function of the desalination plant is to minimize the total annual cost (TAC). The capital and operational costs of each piece of equipment are shown in Table 5 [32,33]. Here, the capital cost of the storage tank (D-1) is negligible in comparison with other units. In order to avoid the phase change occurring the temperature constraint of the solar collector effluent stream (T_6) is set at 95 °C. The product specification (Distillate water flowrate (D)) is set at 2000 kg/h. The mathematical formulation of the problem can be written as:

$$\begin{aligned} &\underset{x\in\Omega}{\text{Minimize}}(\text{TAC}) \\ &\Omega = \{F_{sea}, F_R, A_{SC}, A_{MD}\} \\ &\textit{Subject to} \\ &\quad T_6 < 95^{\circ}\text{C} \\ &\quad D = 2000\,\text{kg/h} \end{aligned} \tag{2}$$

where Ω stands for optimization variables.

The mathematical model of each unit is built on an Aspen Custom Molder (ACM) platform. Feasible Path Successive Quadratic Programming Optimization (FEASOPT) is used to solve the optimization problem which is presented in Eq. (2).

3.3. Optimal results

For a given solar radiation intensity (i.e., $I = 500\ \text{W/m}^2$), we can solve the Eq. (2) and determine the optimal equipment size (which is shown in Table 6) in order to minimize TAC of the desalination plant. The optimal TAC for scanning the solar radiation intensity from 100 to 1000 W/m^2 is shown in Fig. 2. From Fig. 2, the auxiliary electrical heater is not needed when the solar radiation intensity is higher than 500 W/m^2. The solar radiation intensity in the range of 500–1000 W/m^2 fits the design purpose for the fully solar driven AGMD desalination system. For a typical solar radiation curve, this

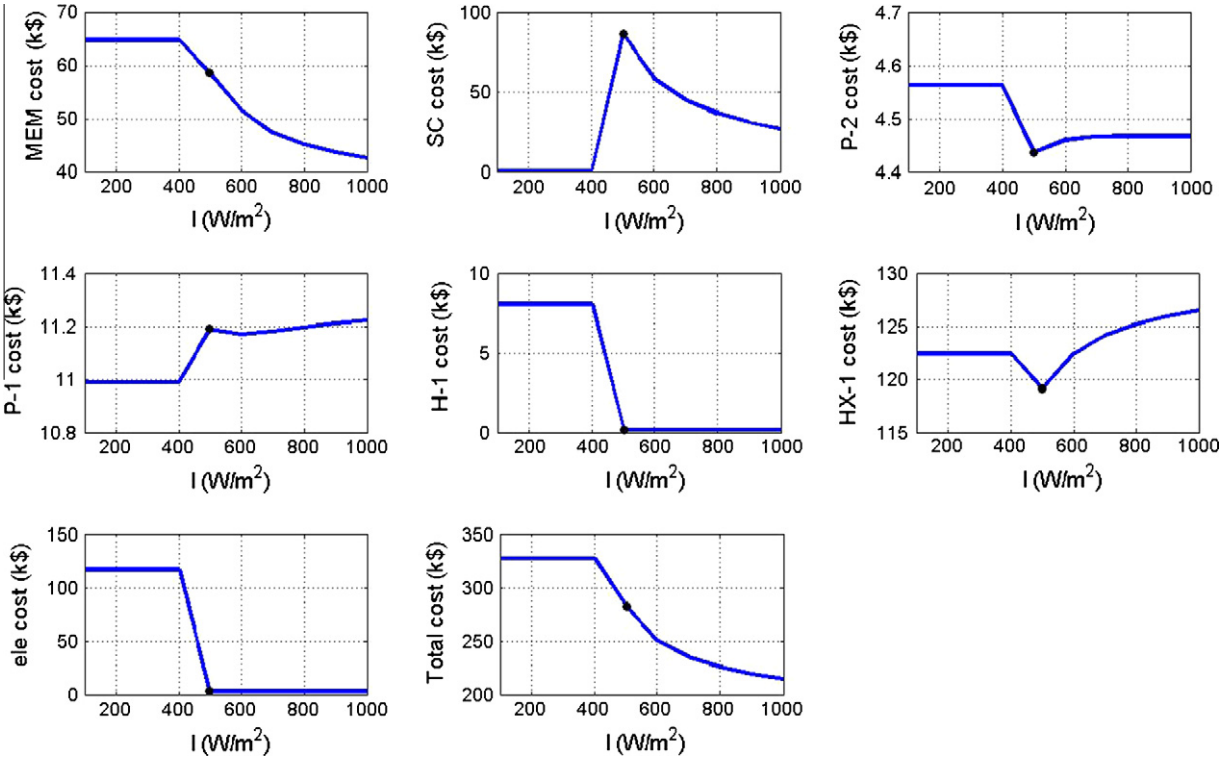

Fig. 2. Optimal TAC vs. solar radiation intensity.

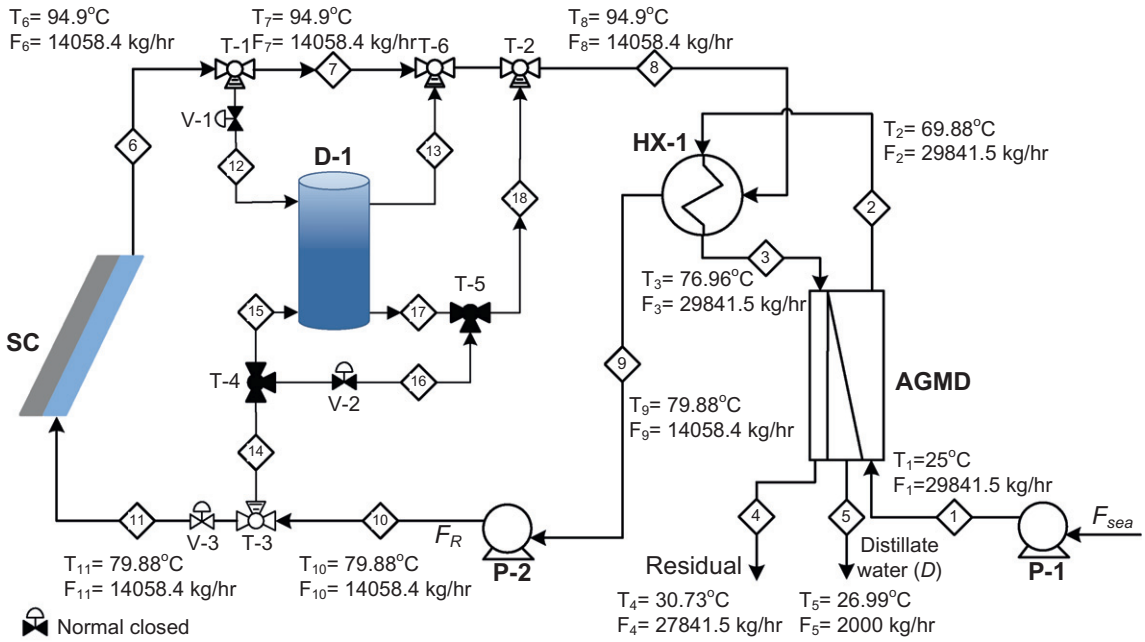

Fig. 3. Optimal operating conditions of solar heated membrane distillation desalination systems.

higher radiation intensity occurs over a short time span. Considering the longer operating time, we chose a solar radiation intensity of 500 W/m^2 as our design basis without auxiliary electrical heater. The dot points shown in Fig. 2 are the optimal design and operating conditions of the desalination plant and are used in the same way in the succeeding figures. The optimal values of all equipment sizes and stream information of the desalination plant are shown in Table 6 and Fig. 3, respectively. The optimal heat exchanger size (A_{HX}) and hot recycled water flowrate (F_R) are 64.4 m^2 and 14058.4 kg/h, respectively. Based on the same distillate water flowrate, the relative values of A_{HX} and F_R are much smaller than in the published design by Banat and Jwaied [11]. The results are shown in Table 6. The reason is that the material for the tube side of the heat exchanger (HX-1) which fills with seawater is titanium which is much more expensive. In order to reduce the capital cost of heat exchanger, the higher temperature of the hot inlet flow is needed to reduce the heat transfer area of HX-1.

4. Sensitivity analysis

After determining the optimal design point of this plant, the next step is to build the control structure for the solar desalination system. The sensitivity analysis is a useful tool to analyze the control pairing for each control loop before constructing the control structure. The control purpose of the plant is to maintain the distillate water flowrate even though the solar radiation intensity varies. The distillate water vapor permeability of the AGMD unit is driven by the temperature difference between the hot and cold side of the membrane. The inlet temperature of the recycled water (T_8) is chosen as our controlled variable. The most interesting thing is to select the manipulated variable for our process. The sensitivity analysis is shown in a later section.

4.1. Seawater flowrate (F_R)

An increased seawater flowrate (F_R) from our optimal design point will cause a decrease in the inlet temperature of the hot seawater with a fixed heat exchange area (HX-1). It will also cause the reduction of the distillate water flowrate (D). On the other hand, a decreased seawater flowrate will cause the reduction of the distillate water flowrate. The simulation result is shown in Fig. 4A. The result shows that the seawater flowrate change will cause a decreased distillate water flowrate and is not suitable as a manipulated variable.

4.2. Recycled water flowrate (F_R)

The recycled water is used as a medium to absorb the solar energy via the solar collector and transfers the heat to cold seawater via the heat exchanger (HX-1). An increased recycled water flowrate will cause an increase in the inlet temperature of the hot seawater with a fixed heat exchange area (HX-1). It will also cause the raising of the distillate water flowrate. Conversely, a decreased recycled water flowrate will cause the phase change of the recycled water stream due to an increased effluent temperature of the solar collector. The simulation result is shown in Fig. 4B. The result shows that the recycled water flowrate change will cause an inoperable situation and is not suitable as a manipulated variable.

4.3. Inlet flowrate of the hot storage tank

In order to maintain the distillate water flowrate, it's preferable to maintain the inlet temperature and flowrate of the hot seawater even if the solar radiation intensity changes. Chang et al. [12] proposed a control scheme which used inlet flowrate of the hot storage tank as a manipulated variable. The liquid level of the storage tank was always kept constant and the inlet and outlet flowrate was the same due to overflow design.

The initial temperature of the storage tank (D-1) in our study is 50 °C. When the solar radiation intensity increases, the effluent temperature of the solar collector (T_6) will be increased. In order to keep the inlet temperature of the hot seawater constant (T_3), the hot inlet flow of the storage tank (F_{12}) is increased and mixed with the stored cold water. The cold outlet flow of the storage tank (T_{13}) is mixed with the storage tank bypass flow (stream 7). It's an effective way to handle the inlet temperature of the recycled water

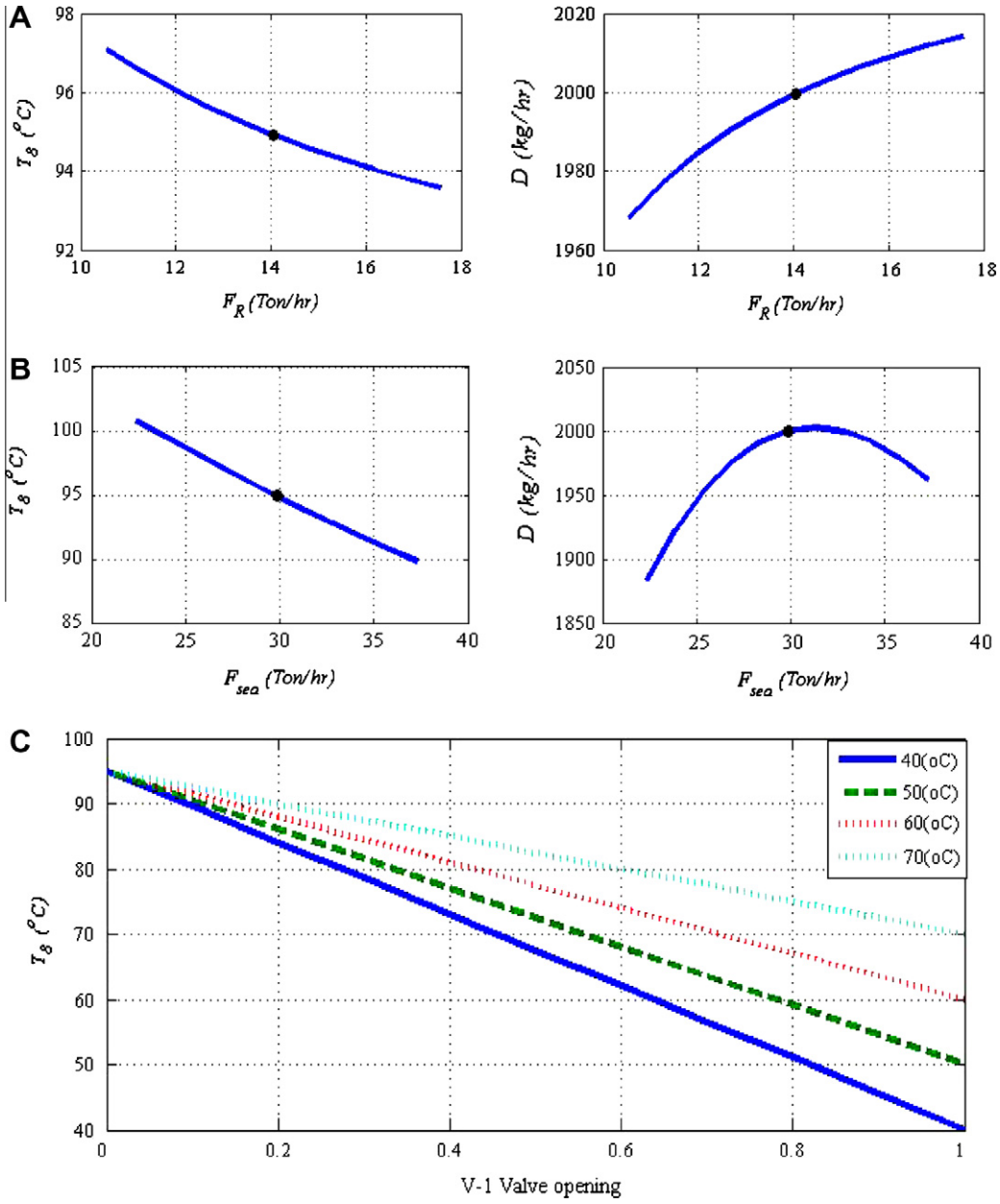

Fig. 4. Steady-state sensitivity analysis: (A) seawater flowrate (F_{sea}), (B) recycled water flowrate (F_R) and (C) inlet flowrate of the storage tank (D-1).

(T_8). The simulation result is shown in Fig. 4C. We chose the inlet flowrate of the hot storage tank as our manipulated variable.

5. Control structure development

The optimal TAC design of the fully solar driven AGMD desalination plant is described in Section 3. However, in a practical situation, the unpredicted solar radiation intensity is a disturbance to our process. In order to achieve a smooth operating distillate water flowrate (D), the control structure is needed to keep the distillate water flowrate constant. From sensitivity analysis, which is presented in Section 4, we can determine the control pairing of inlet temperature of the shell side of the heat exchanger (T_8, controlled variable) and the inlet flowrate of the storage tank (F_{12}, manipulated variable). In this section, we will discuss the tuning of the control parameters and control performance testing under different solar radiation scenarios.

5.1. Structure CS1

The two operating modes of the solar desalination plant are established for handling day and night operation. The control structure 1 of the plant is shown in Fig. 5A. The day and night operating modes are drawn in blue and red colors, respectively. The following control loops are used in CS1:

1. For day operating mode, the inlet temperature of the hot side of the heat exchanger (T_8) is controlled by manipulating the inlet flowrate of the storage tank (F_{12}).
2. For night operating mode, the inlet temperature of the hot side of the heat exchanger (T_8) is controlled by manipulating the bypass flowrate of the storage tank (F_{16}).

For day operating mode, the solar radiation energy is supplied to heat up stream 6. When the T_8 changes, the inlet flowrate of the storage tank (F_{12}) is changed to keep the T_8 constant. When

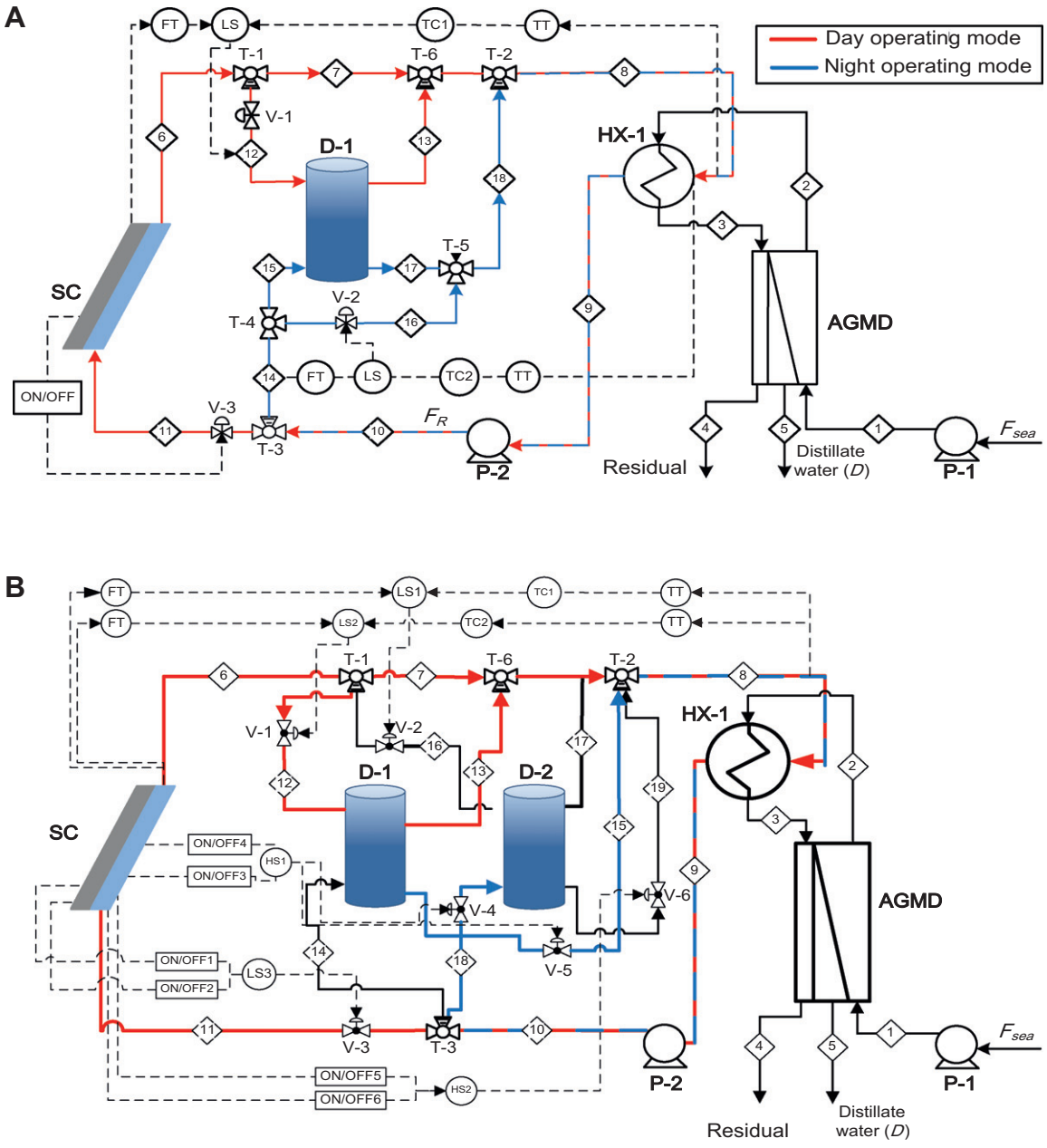

Fig. 5. Control structure developments for the desalination plant: (A) CS1, (B) CS2.

the operating mode of the plant changes from day to night, the temperature difference between the absorbed plate and the fluid in the solar collector is measured and the recycled flowrate (F_{11}) is adjusted to zero. The function of the low switch (LS1) is to select the lower signal between the flowrate of stream 11 (F_{11}) and the temperature controller output (TC1). For night operating mode, there is no flowrate of stream 6 (F_6) which means no inlet flowrate to the storage tank (F_{12}). The recycled flowrate pumps into stream 14. When the T_8 changes, the storage tank bypass flowrate (F_{16}) is changed to keep the T_8 constant. The function of the low switch (LS2) is to select the lower signal between the flowrate of stream 14 (F_{14}) and temperature controller (TC2) output.

5.1.1. Tuning of controller parameters

Three first-order temperature measurement lags of 30 s are used in all temperature control loops. Relay-feedback tests are used to obtain the ultimate gain and frequency. Then the temperature PI controllers are tuned using the Zigler–Nichols tuning rules. The proportional gain and reset time of TC1 are 8.02 (%/%), 86.67 (s), respectively. And 35.41 (%/%) and 87.5 (s) for TC2.

5.1.2. Simulation results

The dynamic simulation result of CS1 is shown in Fig. 6. There are two problems with the dynamic simulation. For a given typical summer solar radiation intensity curve, the temperature of stream 6 (T_6) increases in excess of 100 °C when the solar radiation intensity is larger than 800 W/m^2. This will cause stream 6 to vaporize. The other problem is in night operating mode. When the system turns to night operating mode, the temperature of the storage tank ($T_{D\text{-}1}$) will be decreased due to energy transfer to AGMD module. A decreasing energy supply from the tank will cause a decreasing distillate water generation rate. The results show difficulty in maintaining the distillate water flowrate by using control structure 1.

5.2. Structure CS2

The problems of CS1 are uncontrollable T_6 and $T_{D\text{-}1}$. In order to overcome the control issues of CS1, the modification of CS1 is shown in Fig. 5B. The day and night operating modes are drawn in blue and red colors, respectively. The control loops are used as in CS1. The main differences between CS1 and CS2 are: The CS2 method uses an increased recycled water flowrate compared with the optimal design flowrate and two storage tanks instead of one. We will discuss this in the following section.

5.2.1. Modified optimal operating point

When the solar radiation intensity increases, the optimal design temperature of T_6 will change from 95 °C to in excess of 100 °C. It will cause the vaporization of the stream 6. In order to prevent the vaporizing phenomena, we need to reduce T_6 without changing the size of the desalination plant which will adversely affect the TAC. The sensitivity analysis is used to determine the most sensitive variable of T_6 which is the recycled water flowrate. The result is shown in Fig. 7. If the recycled water flowrate changes from 14,056 kg/h to 140,560 kg/h, the T_6 will change from 95 °C to

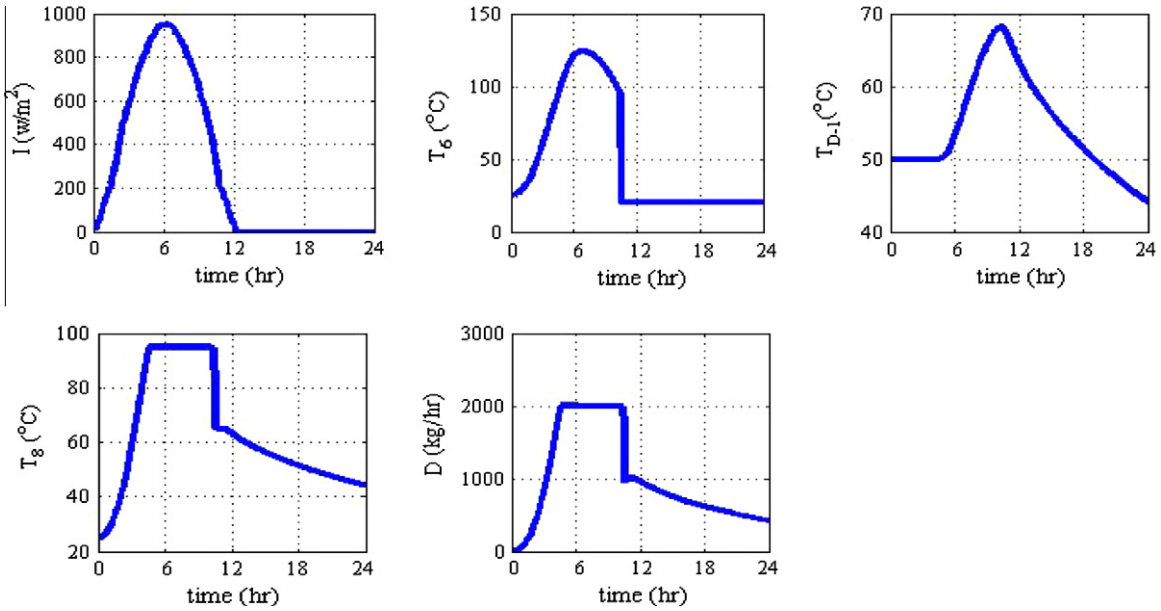

Fig. 6. Dynamic simulation result of CS1.

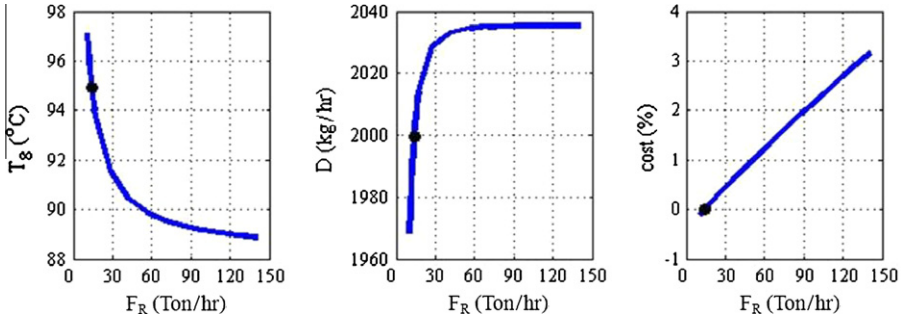

Fig. 7. Modified steady-state operating point of the desalination plant.

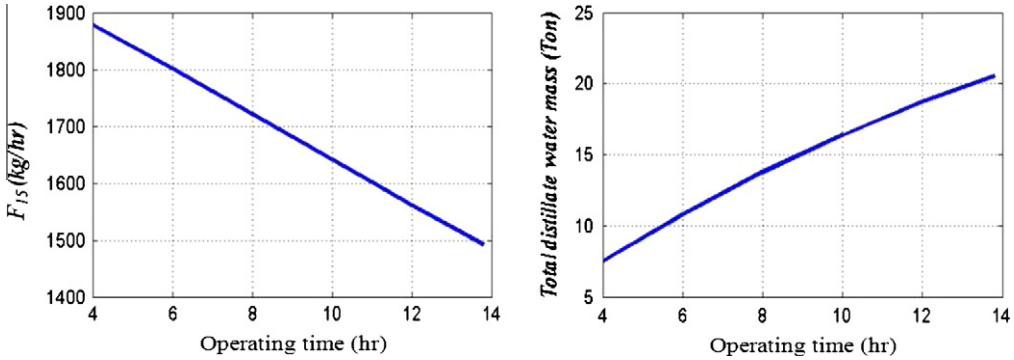

Fig. 8. The outlet flowrate (F_{15}) from the storage tank vs. distillate water flowrate.

88 °C. This change will increase the control operational margin of the desalination plant.

5.2.2. Comparison of the control structures CS1 and CS2

For day operating mode, the control scheme is completely the same with CS1 and CS2. But in order to maintain the stable distillate water flowrate for night operation, the sequential arrangement of two storage tanks is used to maintain the temperature (T_8). Initially, the water is stored, and absorbs energy, in the D-1 tank. When the operating mode turns from day to night, the hot water is supplied from D-1 and flows into the empty tank (D-2). The two storage tanks are used on alternate days. This control scheme is shown in Fig. 5B. The size of the storage tanks will affect their operating temperature during day-time operation because an increase in size can provide larger energy storage capacity. Here, the size is set at 140 m^3 as a reasonable operating volume.

During night operating mode, the hot water (F_{15}) from the storage tank can provide the energy to AGMD unit. F_{15} can be seen as an optimization variable for maximizing the distillate water flowrate. The result is shown in Fig. 8. The operating time from sunset to sunrise is around 14 h. The evacuating time of the storage tank (D-1) can be varied between 4 and 14 h. The optimal flowrate from the storage tank occurs at the end of the operating time; this flowrate and the total distillate water mass are around 1500 kg/h and 21,000 kg, respectively.

5.3. Simulation results

In the last section, we built the CS2 for the desalination plant. The short-term and long-term solar radiation disturbances have to be tested to understand the control performance of the proposed control structure. In short-term disturbance test, Soubdhan et al.

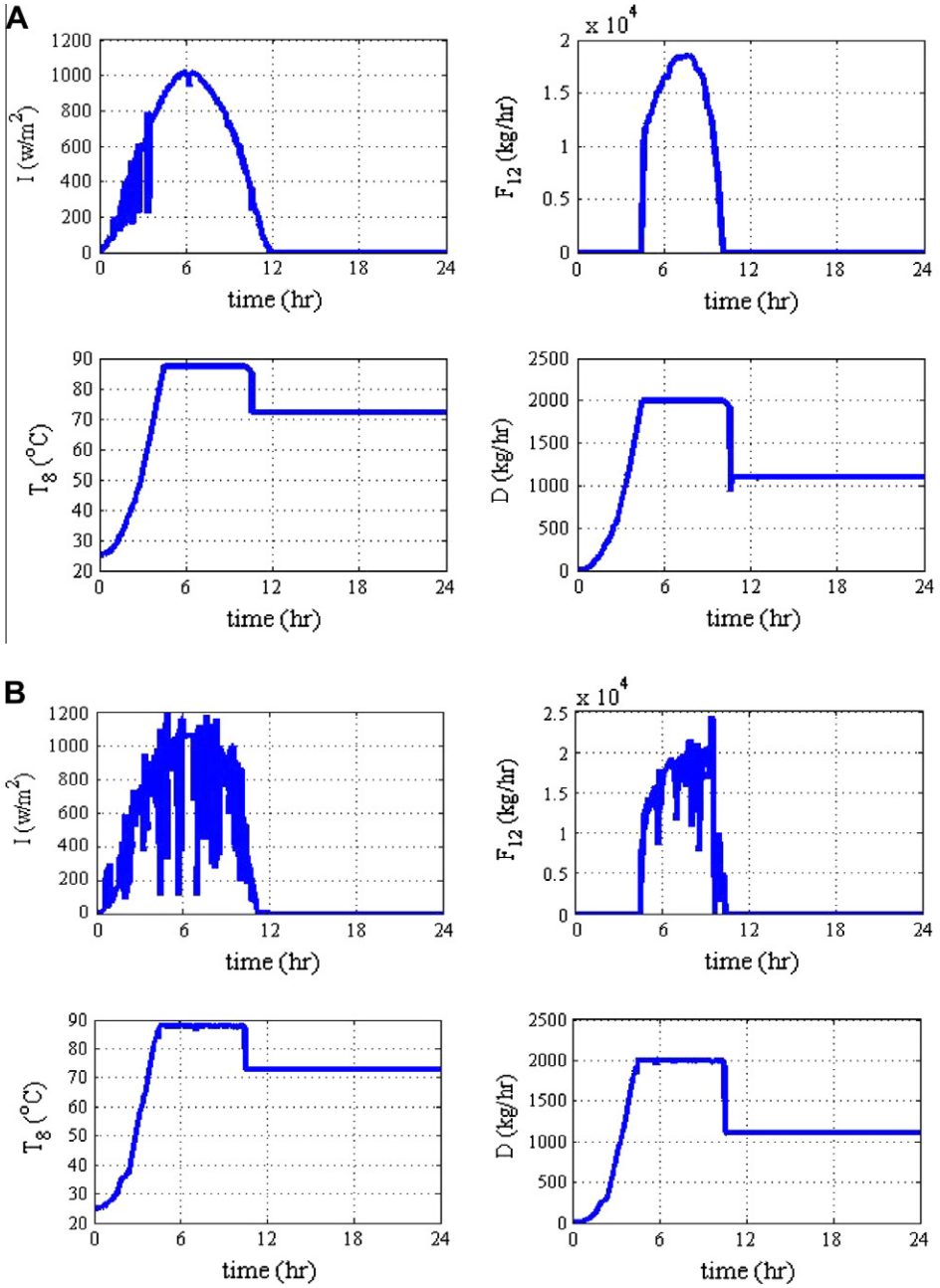

Fig. 9. Control result of the desalination plant for: (A) sunny weather and (B) cloudy weather.

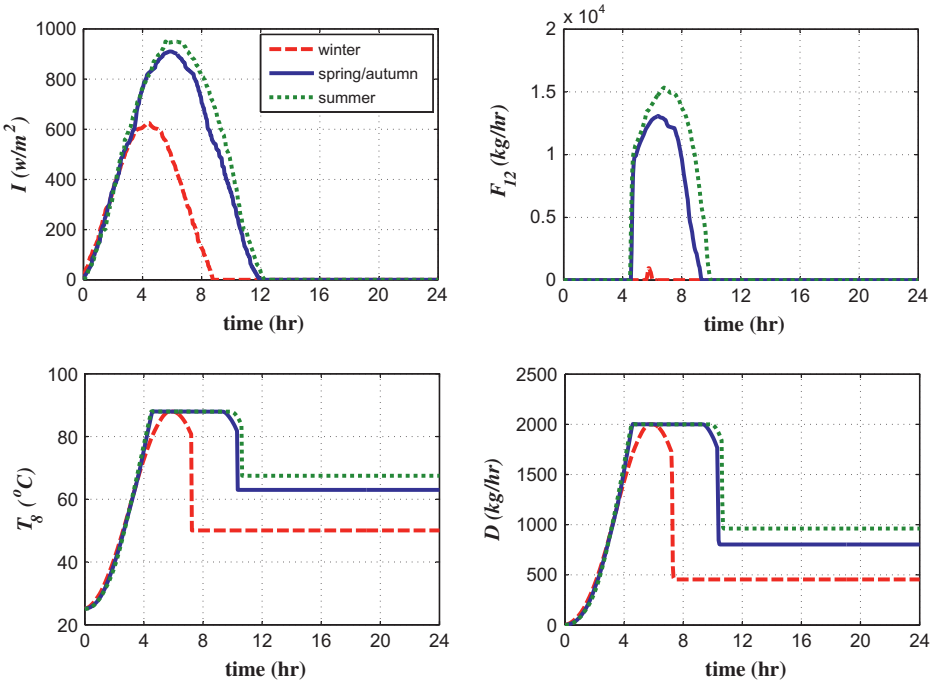

Fig. 10. Control result of the desalination plant for different seasons in Taiwan.

[34] provided solar radiation intensity curves from sunrise to sunset for sunny and cloudy weather in summer and we used the curves as our solar energy sources. The simulation results are shown in Fig. 9. The distillate water flowrate during day and night operation can be maintained at 2000 kg/h and 1100 kg/h. The total distillate water masses during sunny and cloudy weather are 28.62 and 28.22 tons, respectively. In long-term disturbance test, Chang [35] provided typical solar radiation intensity curves for different seasons in Taiwan. The solar radiation intensities of spring and autumn are almost identical and therefore are referenced together in the following text. The simulation results are shown in Fig. 10. The maximum solar radiation intensity in winter is two-thirds the value in summer. All the dynamic responses of the distillate water flowrate can operate at a stable level during day and night operating mode. The heating times which are provided by the solar radiation intensity for spring/autumn, summer, and winter from room temperature to set point temperature of the PI controller are 5, 5, 6.1 h, respectively. The stable operating times during day and night operation of spring and autumn are both 4.7 and 10.4 h, respectively. These times in summer are 6 and 13 h and in winter are 1.8 and 22.3 h. The total distillate water masses of spring/autumn, summer and winter are 26.32, 29.37, 15.89 tons, respectively.

6. Conclusion

In this work, Aspen Custom Molder was used to model and simulate a solar driven desalination plant. We propose a pseudo steady-state method to evaluate and assess the TAC of a time-varying solar desalination plant. The design variables of the system are AGMD membrane area, solar collector area, recycled water flowrate, and seawater flowrate. The objective function of the plant is to minimize the TAC by varying solar radiation intensity. The optimal TAC of the fully solar driven desalination plant is around \$280,000 at 500 W/m^2. The control structure was built to maintain the distillate water flowrate. In order to obtain a wider operating range, a modified operating condition and two storage tanks have been utilitised (CS2). The dynamic simulation of the control structure was completed and the result shows it can maintain the distillate water flowrate at a stable level even during day and night operation. Finally, daily (sunny and cloudy weather) and long term (different seasons) solar radiation intensities have been investigated. The total distillate water masses during sunny and cloudy weather are 28.62 and 28.22 tons which are not significantly different. But the total distillate water masses during spring/autumn, summer and winter are 26.32, 29.37, 15.89 tons due to significant differences in solar radiation intensity.

Acknowledgements

The authors would thank for the financial support for this research project provided by the National Science Council of Taiwan government and the Aspen Technology, Inc. for the use of Aspen Custom Modeler for education and academic researches.

References

[1] Al-Karaghouli AA, Alnaser WE. Experimental comparative study of the performances of single and double basin solar-stills. Appl Energy 2004;77:317–25.
[2] Dev R, Abdul-Wahab SA, Tiwari GN. Performance study of the inverted absorber solar still with water depth and total dissolved solid. Appl Energy 2011;88:252–64.
[3] Fiorenza G, Sharma VK, Braccio G. Techno-economic evaluation of solar powered water desalination plant. Energy Convers Manage 2003;44:2217–40.
[4] Maidment GG, Eames IW, Psaltas M, Lalzad A. Potential application of a flash-type barometric desalination plant powered by waste heat from electric-power stations in Cyprus. Appl Energy 2006;83:1089–100.
[5] Tsilingiris PT. The glazing temperature measurement in solar stills – errors and implications on performance evaluation. Appl Energy 2011;88:4936–44.
[6] Al Suleimani Z, Nair VR. Desalination by solar-powered reverse osmosis in a remote area of the Sultanate of Oman. Appl Energy 2000;65:367–80.
[7] Al-Juwayhel F, El-Dessouky H, Ettoldney H. Analysis of single effect evaporator desalination systems combined with vapor compression heat pump. Desalination 1997;114:253–75.
[8] Zejli D, Ouammi A, Sacile R, Dagdougui H, Elmidaoui A. An optimization model for a mechanical vapor compression desalination plant driven by a wind/PV hybrid system. Appl Energy 2011;88:4042–54.
[9] Al-Ismaily HA, Probert SD. Solar-desalination prospects for the sultanate of Oman. Appl Energy 1995;52:341–68.

[10] Avlonitis S, Hanbury WT, Ben Boudinar M. Spiral wound modules performance an analytical solution: Part II. Desalination 1993;89:227–46.
[11] Banat F, Jwaied N. Economic evaluation of desalination by small-scale autonomous solar-powered membrane distillation units. Desalination 2008;220:566–73.
[12] Chang H, Wang GB, Chen YH, Li CC, Chang CL. Modeling and optimization of a solar driven membrane distillation desalination system. Renew Energy 2010;35:2714–22.
[13] El-Bourawi MS, Ding Z, Ma R, Khayet M. A framework for better understanding membrane distillation separation process. J Membr Sci 2006;285:4–29.
[14] Gude VG, Nirmalakhandan N, Deng S, Maganti A. Low temperature desalination using solar collectors augmented by thermal energy storage. Appl Energy 2012;91:466–74.
[15] Hanemaaijer JH, van Medevoort J, Jansen AE, Dotremont C, van Sonsbeek E, Yuan T, et al. Memstill membrane distillation- a future desalination technology. Desalination 2006;199:175–6.
[16] Kumar R, Umanand L. Modeling of a pressure modulated desalination system using bond graph methodology. Appl Energy 2009;86:1654–66.
[17] Lamei A, van der Zaag P, von Munch E. Impact of solar energy cost on water production cost of seawater desalination plants in Egypt. Energy Policy 2008;36:1748–56.
[18] Wu JW, Hu EJ, Biggs MJ. Thermodynamic cycles of adsorption desalination system. Appl Energy 2012;90:316–22.
[19] Bui VA, Vu LTT, Nguyen MH. Simulation and optimisation of direct contact membrane distillation for energy efficiency. Desalination 2010;259:29–37.
[20] Cabassud C, Wirth D. Membrane distillation for water desalination: how to chose an appropriate membrane? Desalination 2003;157:307–14.
[21] Ben Bacha H, Dammak T, Ben Abdalah AA, Maalej AY, Ben Dhia H. Desalination unit coupled with solar collectors and storage tank: modeling and simulation. Desalination 2007;206:341–52.
[22] Koschikowski J, Wieghaus M, Rommel M. Solar thermal-driven desalination plants based on membrane distillation. Desalination 2003;156:295–304.
[23] Meindersma GW, Guijt CM, de Haan AB. Desalination and water recycling by air gap membrane distillation. Desalination 2006;187:291–301.
[24] Chang H, Lyu SG, Tsai CM, Chen YH, Cheng TW, Chou YH. Experimental and simulation study of a solar thermal driven membrane distillation desalination process. Desalination 2012;286:400–11.
[25] Gálvez JB, García-Rodríguez L, Martín-Mateos I. Seawater desalination by an innovative solar-powered membrane distillation system: the MEDESOL project. Desalination 2009;246:567–76.
[26] Guillen-Burrieza E, Blanco J, Zaragoza G, Alarcon DC, Palenzuela P, Ibarra M, et al. Experimental analysis of an air gap membrane distillation solar desalination pilot system. J Membr Sci 2011;379:386–96.
[27] Song L, Ma Z, Liao X, Kosaraju PB, Irish JR, Sirkar KK. Pilot plant studies of novel membranes and devices for direct contact membrane distillation-based desalination. J Membr Sci 2008;323:257–70.
[28] Reid RC, Prsusnitz JM, Poling BE. The properties of gases & liquids. 4th ed. McGraw-Hill international edition; 1986.
[29] Luyben WL. Design and control degrees of freedom. Ind Eng Chem Res 1996;35:2204–14.
[30] Al-Nimr MA, Kiawn S, Al-Alwah A. Size optimization of convention solar collectors. Energy 1998;23:373–8.
[31] Hollands KGT, Shewen EC. Optimization of flow passage geometry for air-heating, plate-type solar collectors. J Sol Energy Eng 1981;103:323–30.
[32] Seider WD, Seader JD, Lewin DR, Widagdo S. Production and process design principles synthesis, analysis, and evaluation. 3rd ed. John Wiley & Sons, Inc.; 2010.
[33] Peters MS, Timmerhaus KD. Plant design and economics for chemical engineers. 4th ed. New York: McGraw-Hill; 1991.
[34] Soubdhan T, Emilion R, Calif R. Classification of daily solar radiation distributions using a mixture of Dirichlet distributions. Sol Energy 2009;83:1056–63.
[35] Chang TP. Performance evaluation for solar collectors in Taiwan. Energy 2009;34:32–40.